VIBRIOBACTIN MEDIATED BIOFILM FORMATION IN *VIBRIO CHOLERAE*

A Thesis
by
ANTHONY DAVID ANGOTTI

Submitted to the Graduate School
at Appalachian State University
in partial fulfillment of the requirements for the degree of
MASTER OF SCIENCE

August 2013
Department of Biology

VIBRIOBACTIN MEDIATED BIOFILM FORMATION IN *VIBRIO CHOLERAE*

A Thesis
by

ANTHONY DAVID ANGOTTI

August 2013

APPROVED BY:

_____
Dr. Ece Karatan
Chairperson, Thesis Committee

_____
Dr. Mary U. Connell
Member, Thesis Committee

_____
Dr. Theodore Zerucha
Member, Thesis Committee

_____
Dr. Sue Edwards
Department Chair, Department of Biology

_____
Dr. Edelma Huntley
Dean, Research and Graduate Studies

Abstract

VIBRIOBACTIN MEDIATED BIOFILM FORMATION IN *VIBRIO CHOLERAE*
(August 2013)

Anthony David Angotti
B.S., Allegheny College
M.S., Appalachian State University

Thesis Chairperson: Ece Karatan

Vibrio cholerae transitions between a free-swimming planktonic lifestyle and a multicellular community called a biofilm, which is used as protection from environmental stressors. Biofilm formation is influenced by a number of factors and can be up-regulated by the polyamine norspermidine. Norspermidine also forms the backbone of the siderophore vibriobactin, which is secreted in response to iron deficient conditions. The dual role of norspermidine as a biofilm signaling molecule and a key component of vibriobactin suggests that there is a link between norspermidine synthesis, biofilm formation, and environmental iron concentrations.

The objective of this study was to analyze the role of vibriobactin in biofilm formation. These analyses utilized mutants defective in vibriobactin transport (*viuA::tet*^{R}) or synthesis (Δ*vibF*) and were assayed in iron-replete (EZRDM) and -deplete (100 µg/ml EDDA) conditions. Our results show that biofilm cell density is significantly different between wild-type *V. cholerae*, *viuA::tet*^{R}, and Δ*vibF* over a period of 1-3 days in iron-replete and -deplete media. Confocal microscopy experiments using STYO-9 show that

biofilm architecture and maturation is altered substantially in both *viuA::tet*^{R} and Δ*vibF* mutants compared to wild-type under iron-replete and -deplete conditions over a period of 1-3 days. Furthermore, competition indices show that *viuA::tet*^{R} is outcompeted for space in biofilms by wild type and Δ*vibF* is at a competitive advantage. Confocal microscopy experiments show that *viuA::tet*^{R} and Δ*vibF* have unique distributions in biofilms when mixed with wild type.

Acknowledgements

I would like to thank a number of people who made this research possible. Firstly, I would like to thank Paula Watnick and Steve Calderwood who generously provided me with the *Escherichia coli* to synthesize the vibriobactin mutant strains. Also, I would like to acknowledge Joe Harrison and Matt Parsek for generously providing the mCherry plasmid used in this study. Matthew Swain also provided me with a great deal of assistance towards the statistical analyses. Thanks also go to the Office of Student Research for providing funding towards this project, and the graduate school for providing me with a North Carolina tuition waiver to attend Appalachian State University.

I would like to extend my thanks to my committee members, Dr. Ted Zerucha and Dr. Mary Connell, for their support and guidance throughout my studies at Appalachian State University. Also I am happy to acknowledge all members of the Karatan Lab that helped make the long hours in the lab worth it. My friends and family were also a tremendous support group, and without them I would have never been able to reach this level of achievement. Finally, but most certainly not least, I would like to thank my adviser Ece Karatan. Her support and guidance has helped me grow as a student, scientist, and person. She embodies what it means to be a mentor.

Table of Contents

List of Tables

List of Figures

Introduction

The relationship with iron is one of conflict for most bacteria. Iron is necessary for a number of cellular processes including the tricarboxylic acid cycle and DNA metabolism [1]. Although iron is necessary for bacteria it can also be toxic. When iron is in excess it results in the Fenton Reaction, which causes free hydroxyl radicals (Figure 1) [2]. These free hydroxyl radicals result in the destruction of DNA, an increase in mutagenesis, and increased sensitivity to H_2O_2 [3].

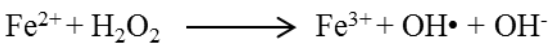

Figure 1. Fenton's Reaction generates free hydroxyl radicals

Due to these reasons iron levels inside the cell are closely managed and can regulate a large number of processes. Although iron is the fourth most abundant element in the earth's crust it is in very short supply due to its insolubility at physiological pH. When ferrous iron (Fe^{+2}) reacts with oxygen it oxidizes into its ferric state (Fe^{+3}) which is insoluble at non-acidic pH. This process occurs by iron binding to oxygen to fill its octet resulting in insoluble Fe_2O_3. The only time iron is available in its ferrous state is at acidic pH and anaerobic conditions. This is due to iron binding negatively charged groups of an acid to maintain its dissolved Fe^{+2} state. An example of the Fe^{+2} state would be in the presence of hydrochloric acid where it can bind to two molecules of chlorine and form

ferrous chloride. Since it is insoluble at non-acidic pH it is unavailable to most bacteria for use as free iron [2].

Supplies of iron in a human host, despite being present in amounts up to five grams per person, are almost completely unavailable to bacteria for use as free soluble iron. Most iron in the body is found in the form of hemoglobin while the rest is protected by other compounds including heme, ferritin, lactoferrin, and transferrin [4]. In order to acquire iron tied up in these protective molecules bacteria have developed mechanisms to steal it from their host. *Vibrio cholerae*, the causative agent of the acute diarrheal disease cholera, possesses a number of iron acquisition mechanisms to thrive in the intestines of human hosts, and to survive in an aquatic environment where soluble iron is also in short supply. The most notable of these mechanisms include Hut proteins that can utilize heme as a source of iron, a FhuABCD system that can acquire iron from the fungal compound ferrichrome, and the use of siderophores [1] (Figure 2).

Siderophores are low molecular weight high affinity ferric iron chelators that are synthesized by bacteria and some fungi when iron is limited in the environment [5]. Iron-limited conditions are encountered frequently since, in an aquatic environment, most iron is insoluble and in a host organism iron is fiercely protected. Siderophores come in a variety of forms with the predominant two being the hydroxamate and catecholate varieties. Hydroxamate siderophores include ferrichrome which is produced by many fungi and desferrioxamine from a variety of bacteria including *Streptomyces* [6,7].

Catecholate siderophores are produced by Gram-negative bacteria and include the *Escherichia coli* siderophore Enterobactin and the *V. cholerae* siderophore vibriobactin [8]. There are also a variety of siderophores termed mixed because they fit

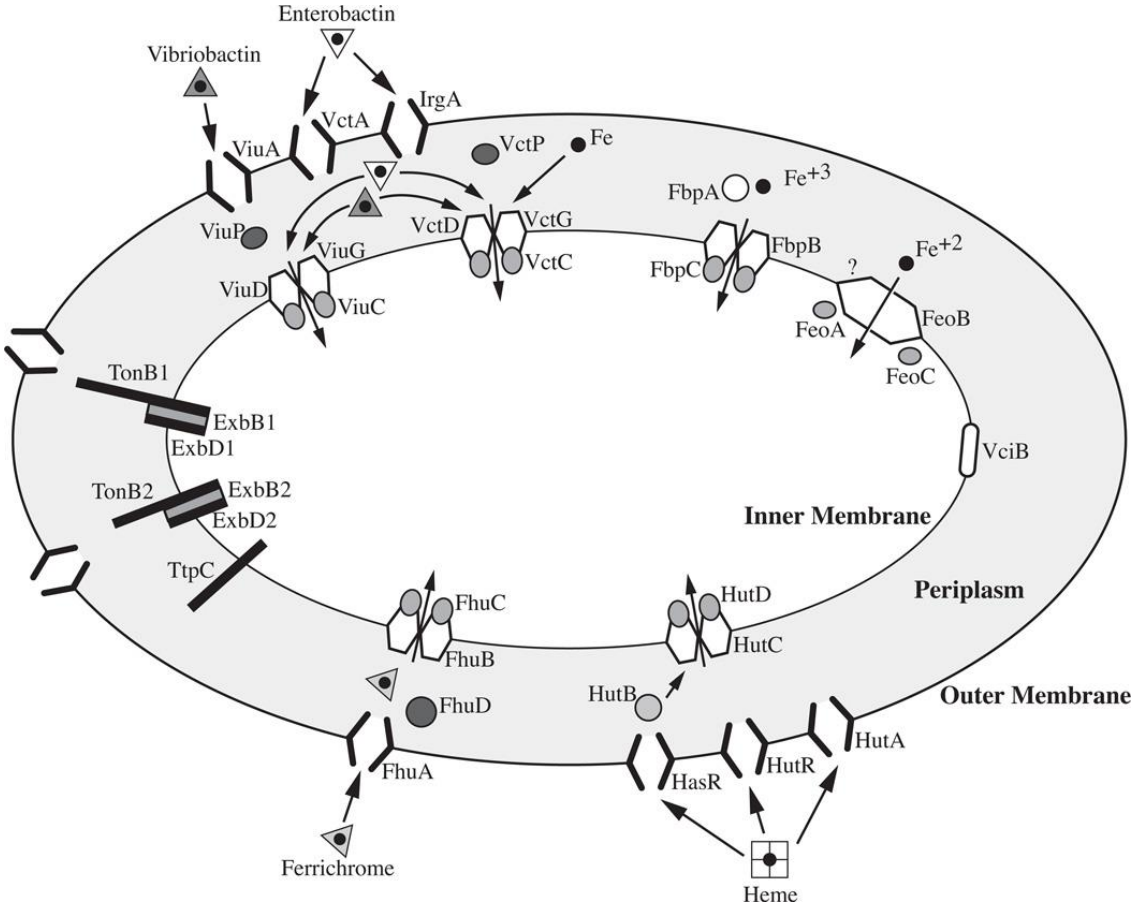

Figure 2. *V. cholerae* iron acquisition systems utilize free ferrous or ferric iron, Vibriobactin, Enterobactin, Heme, and Ferrichrome. [1]

into neither category. These include pyoverdine which is synthesized by *Pseudomonas aeruginosa* [9].

There are many systems of iron acquisition, but siderophores are one of the most useful for bacteria when in a host organism due to their higher affinity for iron than the host systems. Most siderophores have a higher affinity for iron than the human iron containing compounds lactoferrin, heme, ferritin, and transferrin [10,11]. Also, since most bacteria in the body coexist with other species they have developed systems to

acquire foreign siderophores, called xenosiderophores [12,13,14,15]. Since iron can be toxic to cells at high concentrations, mechanisms have been developed by bacteria to regulate the secretion and uptake of siderophores. All known siderophore systems are repressed at high levels of iron, but activated at low iron levels. Typically this result is due to the repressor Fur, the central regulator of iron-dependent processes in Gram-negative bacteria [16,17].

When iron is limited in the environment Fur will signal *V. cholerae* to begin assembling vibriobactin from its precursor molecules. To assemble vibriobactin three different proteins are utilized to combine three molecules of 2,3-dihydroxybenzoate (DHBA), the polyamine norspermidine, and two L-threonine molecules into vibriobactin. Two of the proteins, VibB and VibH, act predominately as carrier proteins to carry necessary precursor molecules through the vibriobactin formation process. The third protein, VibF, acts as the primary assembly protein for vibriobactin by tethering one molecule of DHB and two oxazoline rings to norspermidine (Figure 3) [18].

Many bacteria, including *V. cholerae,* transition between an individual life stage and a multicellular community called a biofilm. These multicellular communities provide *V. cholerae* with increased resistance to environmental stressors like antibiotics and high acid concentrations [19,20]. Interestingly the backbone molecule of vibriobactin, norspermidine, also acts as a signaling molecule that upregulates biofilm formation [21] (Figure 4).

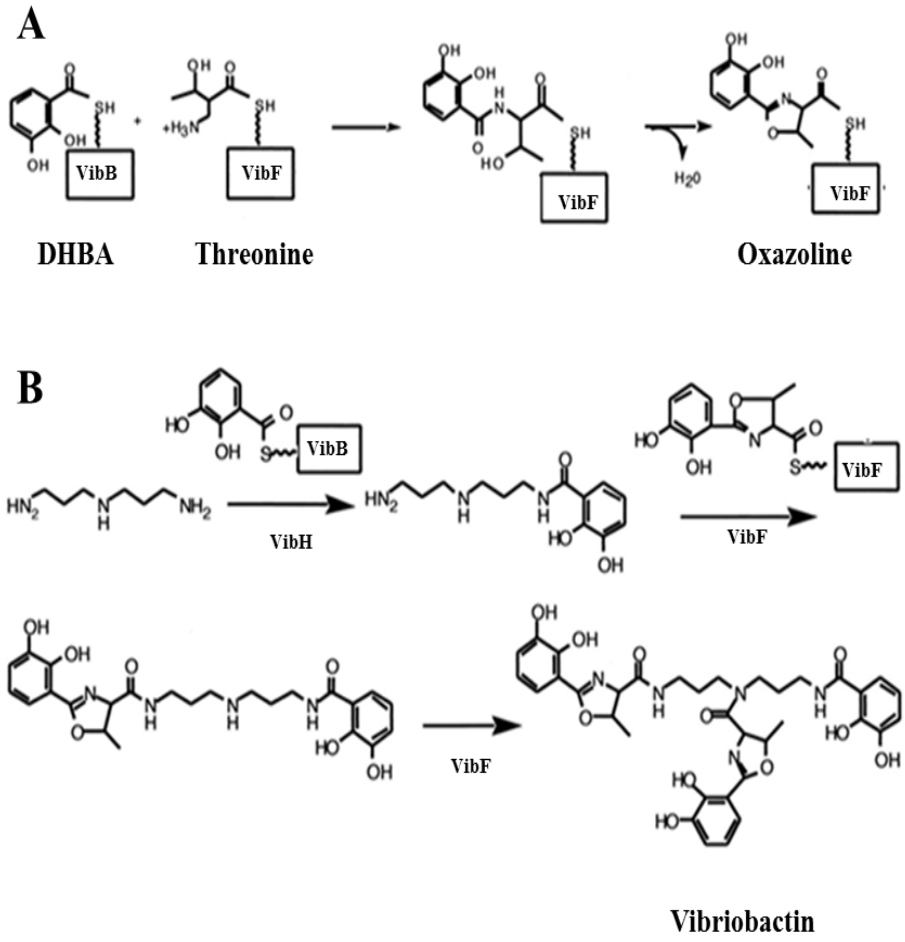

Figure 3. Assembly of oxazoline rings (A) and vibriobactin (B) by VibB, VibF, and VibH.

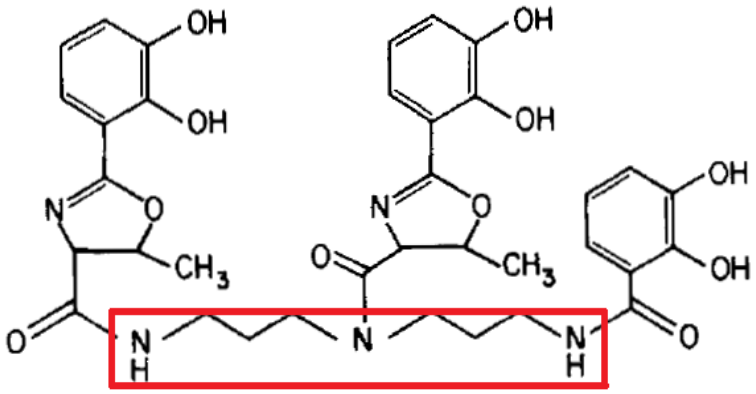

Figure 4. Vibriobactin contains the biofilm signaling molecule norspermidine as its backbone. Norspermidine is boxed in the image above.

In addition to norspermidine many signals and conditions can influence biofilm formation. Iron and iron acquisition systems have been shown to be powerful regulators of biofilm formation in various microorganisms including *P. aeruginosa, E. coli, Staphylococcus aureus, Mycobacterium smegmatis,* and many others [22,23,24,25].

Free iron concentration has been shown to impact biofilm formation in some strains of *V. cholerae*. When exposed to increasing concentrations of the ferric iron chelator Ethylenediamine-N, N'–diacetic acid (EDDA) biofilm formation was drastically reduced in *V. cholerae* O1 El Tor. At an EDDA concentration of 50 µg/ml biofilm formation of wild-type *V. cholerae* was decreased by nearly 70% compared to wild type grown in unchelated media [26]. Although the vibriobactin acquisition system has not yet been tied to biofilm formation in *V. cholerae,* siderophores have been shown to be important to biofilm formation in other bacteria, namely *P. aeruginosa* [22]. The importance of free iron to biofilm formation of *V. cholerae* and other bacteria combined

with the presence of the biofilm signaling molecule norspermidine as the backbone of vibriobactin led us to hypothesize that the vibriobactin iron uptake system was likely important in biofilm signaling and maturation.

The objective of this work was to determine if a deletion of the vibriobactin synthesis gene, *vibF,* and the vibriobactin uptake gene, *viuA,* impacts biofilm maturation in both iron-rich and –deplete conditions. The second objective of this work was to determine if the deletion of these genes impacted how *V. cholerae* competes with wild type cells in mixed biofilms.

Materials and Methods

Bacterial strains, plasmids, media, and reagents.

Bacterial strains used in this study are listed in Table 1 and primers in Table 2.

Table 1. Strains and Plasmids

Strain/Plasmid	Genotype	Reference
***E. coli* strains**		
PIW297	SM10 *α λ pir* w/pPAC20, Amp^r, Km^r Tc^r	[27]
PIW298	SM10 *α λ pir* pWCW3, Amp^r Km^r	[27]
***V. cholerae* strains**		
PW357	MO10 *lacZ::vpsLp→lacZ*, Sm^r	[28]
PW249	MO10, clinical isolate of *V. cholerae* O139 from India, Sm^r	[29]
AK299	PW357 pSMC2::GFP, Sm^r	[30]
AK303	MO10 *viuA*::*tet*^{r} Sm^r, Tc^r	This Study
AK310	MO10 Δ*vib*F, Sm^r	This Study
AK353	AK303 pUCP18::mCherry, Sm^r, Amp^r	This Study
AK354	AK310 pUCP18::mCherry, Sm^r, Amp^r	This Study
Plasmids		
pSMC2	pMUT2 (GFP) containing 1.8-kb stabilizing fragment from pUCP181.8; Amp^r $Carb^r$	[31]
pUCP18::mCherry	Putitutive mCherry expression vector Amp^r/$Carb^r$	[32]
pWCW3	pCVD442 with *Sal*I-*Sac*I fragment from Pwcw2 containing 882-bp in-frame deletion of *vibF*; Amp^r	[33]
pPAC20	pCVD442 with 4.2-kbp PvuII fragment containing *viuA::Tc*^{r}; Amp^r Tc^r	[34]

Table 2. Primers

Primer	Description	Sequence
PA209	Forward primer for *vibF*	5'-GTGTTGGCTGCGTTCGTGAC -3'
PA210	Reverse primer for *vibF*	5'-GGGGTCAGTGGCATCTCCTG-3'
PA219	Forward primer for PBR322 (tet^R in AK303)	5'- CACCGTCACCCTGGATGCTG-3'
PA220	Reverse primer for PBR322 (tet^R in AK303)	5'- TGGTCGTCATCTACCTGCC-3'
PA223	Forward primer for *viuA*	5'- CGCAAACAGCGGGTATGATC-3'
PA224	Reverse primer for *viuA*	5'- AAGGCTAGTCCTGCCCCACTC-3'

Strains were grown on Luria-Bertani (LB) (1% Tryptone, 0.5% Yeast Extract, 85 Mm NaCl) agar with relevant antibiotics for 24 hours at 37°C before being incubated in liquid LB Media with relevant antibiotics. For use in iron assays EZ Rich Defined Medium (EZRDM) was used and was purchased from Technova (Hollister, CA). EZRDM was prepared by company specifications. Antibiotics used in this study were used at the following concentrations unless otherwise stated: streptomycin (100 µg/ml), tetracycline (2.5 µg/ml), ampicillin (50 µg/ml).

To create iron-deplete conditions the ferric iron chelator EDDA was added to EZRDM at desired concentrations and allowed to incubate at 4°C overnight. EDDA used in this study was purchased from Sigma (St. Louis, MO) and deferrated prior to use by method of Rogers as follows: a solution of 80 ml 1N HCl and 5g EDDA was boiled until EDDA dissolved completely then allowed to boil for an additional five minutes; the solution was cooled and vacuum filtered through blotting paper, 703 (VWR International, Radnor, PA #28298-030) using a Buchner funnel; the filtrate was diluted with 750 ml of

cold acetone and the solution was adjusted to a pH of 6 with 10 N NaOH [35]. The pH was measured with BDH test strips (VWR International, #BDH35309-606). After adjusting the pH the solution was allowed to stand overnight at 4° C. The next day, crystals formed in the acetone and the solution was filtered through a Buchner funnel with blotting paper. The filtrate was discarded and the crystals were washed a second time with ice cold acetone. After washing the crystals were dried for 20 minutes at 37° C. Crystals were then stored in a sterile 50 ml conical tube until use.

Construction of Vibriobactin Mutants

Two vibriobactin uptake and synthesis mutants were constructed using double homologous recombination and sucrose. The mutant strain AK303 was defective in vibriobactin uptake as a result of an interruption of the gene encoding the outer membrane vibriobactin uptake protein with a tetracycline resistance cassette; this strain was denoted *viuA*::*tet*^{R}. Another mutant strain, AK310, was constructed by deleting a portion of the key vibriobactin synthesis gene, *vibF*, and was denoted Δ*vibF*. *E. coli* containing the plasmid for *viuA*::*tet*^{R} was plated on tetracycline (2.5 µg/ml) and ampicillin (50 µg/ml) LB plates and incubated overnight at 37°C. Briefly, *E. coli* containing the plasmid with the deletion construct for *vibF* was plated on ampicillin (50 µg/ml) and incubated overnight at 37° C. Wild type *V. cholerae* O139 was grown overnight at 37°C on LB plates containing streptomycin (100 µg/ml). Then *V. cholerae* and *E. coli* containing the plasmids for the construction of either *viuA*::*tet*^{R} or Δ*vibF* were

mated on LB agar plates without antibiotics and incubated at 37°C overnight. Once mating was complete, half of the overnight growth was streaked for isolation on selection agar containing streptomycin (100 µg/ml) and ampicillin (50 µg/ml) and incubated overnight at 37°C to select for single crossover events. After selecting for bacteria carrying the crossover, four single colonies were streaked for isolation on LB plates containing streptomycin (100 µg/ml) and ampicillin (50 µg/ml) to purify the colony and incubated overnight at 37°C. Next, colonies were streaked for isolation on LB plates without antibiotic to promote a second recombination event in order to delete the vector sequence which includes the sucrose suicide gene, *sacB,* and the ampicillin resistance gene and incubated overnight at 37°C. Subsequently, four colonies were streaked for isolation on sucrose plates (5 g Tryptone, 2.5 g Yeast Extract, 7.5 g agar, and 10% sucrose) and allowed to incubate at room temperature for two days. After incubation individual colonies were patched on selection LB agar to confirm that the ampicillin resistance was properly removed and streptomycin LB agar. The agar to confirm the removal of ampicillin resistance contained streptomycin (100 µg/ml) and either tetracycline (2.5 µg/ml) or ampicillin (50 µg/ml) in the case of *viuA*::*tet*^{R} or ampicillin (50 µg/ml) in the case of Δ*vibF*. Colonies that were selected to have the desired mutation were confirmed by colony PCR with primers indicated in Table 2.

To confirm that the Δ*vibF* strain was defective in producing vibriobactin it was assayed using a Chrome Azurol S (CAS)-Agar Plate Assay. CAS agar was prepared following the recipe of Louden *et al.* [36]. Three percent (w/v) 8-hydroxyquinoline was

used to confirm that plates were functional and producing the characteristic orange halo. Strains were initially grown overnight in LB at 37°C with relevant antibiotics. Then the strains were plated by pipetting liquid culture onto sterile filter paper on the CAS agar plates. When a siderophore is being produced an orange halo will be present on the blue agar surrounding the bacterial colonies. This orange halo is present when any strong iron chelator, like vibriobactin, removes iron from being trapped in the hexadecyltrimethylammonium bromide (HDTMA) dye complex.

Both mutants and the wild type were assayed for growth in EZRDM over 9 hours from 25 ml cultures initially inoculated from overnight culture. The overnight culture cell density was measured with a Bio-Rad 680 microplate reader (Hercules, CA) at 595 nm. The strains were diluted to an optical density of 0.02 in 25 ml. Growth measurements were taken at 595 nm using a BioRad 680 microplate every 30 minutes.

Construction of mCherry Strains

First, *viuA::tet*^{R} and Δ*vibF* were made electrocompetent. Then 50 µl of each electrocompetent mutant was mixed with 2 µl of pUCP18::mCherry in an electrocuvette. The electrocuvette was then electroporated using a Bio-Rad micropulser (Hercules, CA). After electroporation 1 ml of super optimal broth with catabolite repression (SOC) (0.5% Yeast Extract, 2% Tryptone, 10 Mm NaCl, 2.5 Mm KCl, 10 Mm MgCl2, 10 Mm MgSO4, 20 Mm, Glucose) media pre-warmed to 37°C was added to the electroporated cells. The cells were allowed to recover for three hours in SOC media at 30°C. After

recovery the cells were plated on ampicillin (50 mg/ml) LB-agar and were tested for mCherry expression by confocal microscopy.

Confocal Microscopy

A single bacterial colony was grown overnight in 3 ml EZRDM at 37°C. Then the optical density was measured using 150 µl of overnight culture in a 96-well microplate at 595 nm in a model 680 Bio-Rad microplate reader. Overnight cultures were then diluted to an optical density of 0.02 in 10 ml of either EZRDM or EZRDM with 100 µg/ml EDDA. Once inoculated, a 50 mm sterile glass cover slip with a thickness of 0.13 to 0.17 mm (VWR International #48393081) was placed in the conical tube to present a surface for biofilm formation. Cells were then allowed to incubate for 24 and 72 hours at 27°C.

Once the biofilms were incubated for the desired period of time the slide was removed and placed in a sterile 50 ml conical tube. In the conical tube, the biofilm was washed twice with phosphate-buffered saline (PBS) (137 Mm NaCl, 2.7 Mm KCl, 10 Mm Na_2HPO_4, and 2 Mm KH_2PO_4, pH 7.4). After the second wash, 12 ml PBS was added to where it completely covered the biofilm, and then 400 µl of SYTO-9 stain (Excitation: 482 Emission: 500) (Invitrogen, Grand Island, NY) , diluted 3:1000 in water, was added to stain the cells. After SYTO-9 addition the biofilm was incubated in the dark at room temperature for 30 min.

When incubation was complete the cover slip was washed once with PBS and placed on a concave glass slide containing 60 µl EZ-RDM in the well. Once the slide was

placed over the well it was sealed with clear nail polish and the outer surface was sterilized with 100% ethanol. The prepared and sterilized slide was then viewed using a Zeiss LSM 510 Confocal Laser Scanning Microscope. Biofilms were viewed at 20x with an argon laser at 11% power. Z-Stacks were taken with a scan time of 2 at 1024x1024 resolution. Biofilm thickness was estimated using the thickness of the Z-Stack. The biofilm was initially scanned visually to determine an image field representative of the total sample. The image was taken in the center of the biofilm below the air-broth interface. Each experiment was performed with three biological replicates and one representative field was imaged per replicate after visually scanning the entire biofilm. Thicknesses were calculated visually using the Z-stack from the site of attachment to the glass to the top of the tallest microcolony extending from the glass cover slip.

Biofilm Assays

Biofilms were performed in three biological replicates, with three technical replicates each, prepared as previously described with the following modifications [21]. A single bacterial colony was grown overnight in 3 ml EZ-RDM at 37° C. Then the optical density was measured using 150 µl of overnight culture in a 96-well microplate at 595 nm in a model 680 Bio-Rad microplate spectrophotometer. Biofilm samples were then diluted from overnight cultures to an optical density 595 of 0.02 in 300 µl of either EZRDM or EZRDM with 100 µM EDDA and allowed to incubate for 24-72 hours at 37°C. After the desired incubation period planktonic cells were harvested and the biofilm

cells were washed with PBS. One hundred and fifty µl of the unstained planktonic cells were saved to be analyzed with spectrophotometry.

After washing and removing planktonic cells, biofilm cells were treated with 1% (v/v) crystal violet solution and allowed to incubate for 30 min. When the incubation period was complete the unused stain was removed and the biofilm was washed with PBS. After washing, dimethyl sulfoxide (DMSO) (Thermo Scientific, Scientific Fair Lawn, N.J.) was added to solubilize the stained biofilm and the optical density of 150 µl of sample was measured with a model 680 microplate reader (Bio-Rad, Hercules, CA) at 595 nm to quantify the biofilm cell density. To standardize, a control test tube with media but no cells was used to determine background stain. This value was subtracted from the optical density of the biofilm sample stained with crystal violet to determine how much absorbance was a result of the biofilm.

Competition Biofilm Assays

Biofilms were prepared as previously mentioned with the following differences. Wild type and either *viuA::tet*^{R} or Δ*vibF* were mixed 1:1 prior to addition to the biofilm tube. Prior to mixing, each strain was grown from a single colony overnight at 37°C. The overnight culture cell density was measured with a BioRad 680 microplate reader at 595 nm. Prior to mixing, the strains were diluted to an optical density of 0.02. After mixing, the strains were serially diluted to 10^{-7} and 10^{-8} in LB and 90 µl of each dilution was plated on LB plates with relevant antibiotics and counted after incubation for 24 hours at

37°C to determine an input ratio. Competition biofilms were incubated for 24 and 72 hours at 27°C.

After incubation, planktonic cells were extracted, diluted to concentrations of 10^{-7} and 10^{-8}, and plated on LB-X-Gal (5-bromo-4-chloro-3-indolyl-β-D-galactopyranoside) (40 µg/ml) (Gold-Bio, St. Louis, MO) plates with relevant antibiotics for counting. Once planktonic cells were isolated the biofilm was washed with 400 µl PBS and dispersed with 1.0 mm glass beads (Biospec, Battesville, OK) in PBS. The ground biofilm was then serially diluted to 10^{-7} and 10^{-8} in LB and 90 µl of each dilution was plated on LB-Xgal plates for counting. After counting both planktonic and biofilm cells on LB-Xgal plates, competitive indices were calculated by dividing the mutant to wild-type ratio of the competition biofilms with the mutant to wild type ratio of the initial inoculum (Figure 5).

$$\frac{Number\ of\ mutant\ colonies\ post\ incubation}{Number\ of\ wild\ type\ colonies\ post\ incubation} = Competitive\ Index$$

Figure 5. Equation for Competitive Index Calculation

Confocal Biofilm Competition Assays

A single bacterial colony was grown overnight in 3 ml EZ-RDM at 37°C. The optical density was measured using 150 µL of overnight culture in a 96-well microplate at 595 nm in a model 680 Bio-Rad microplate reader. Overnight cultures were diluted to an optical density of 0.02 in 10 ml of either EZRDM or EZRDM with 100 µg/ml EDDA.

Then the diluted strains were mixed 1:1 in a 50 ml conical tube. Once mixed, a 50 mm sterile glass cover slip with a thickness of 0.13 to 0.17 mm (VWR International #48393081) was placed in the conical tube to present a surface for biofilm formation. Cells were then allowed to incubate for 24 and 72 hours at 27°C.

Once the biofilms were incubated for the desired period of time the slide was removed and placed in a sterile 50 ml conical tube. In the conical tube, the biofilm was washed twice with phosphate-buffered saline. Then the cover slip was placed on a concave glass slide containing 60 µl EZ-RDM in the well. Once the slide was placed over the well it was sealed with clear nail polish and the outer surface was sterilized with 100% ethanol. The prepared and sterilized slide was then viewed using a Zeiss LSM 510 Confocal Laser Scanning Microscope. The biofilms were imaged with an argon laser at 80% and helium neon lasers at 5%.

Statistical Analysis

All statistical analyses were done using the program JMP10 to perform two way anova analyses and Student's T-Tests. P-values less than 0.05 were considered significant.

Results

Mutations in viuA and vibF were successfully constructed

To confirm that *vibF* was properly deleted on the a 1.5 kbp portion of the wild type chromosome containing *vibF* was analyzed using PCR. The deletion removed 849 nucleotides within the *vibF* gene resulting in a 651 base-pair region that would be amplified by the PCR primers. The wild type had a 1.5 kbp band which indicated an intact *vibF* gene and the Δ*vibF* strain showed a band between 1 kbp and 0.5 kbp indicative of the 849 base pair removal (Figure 6).

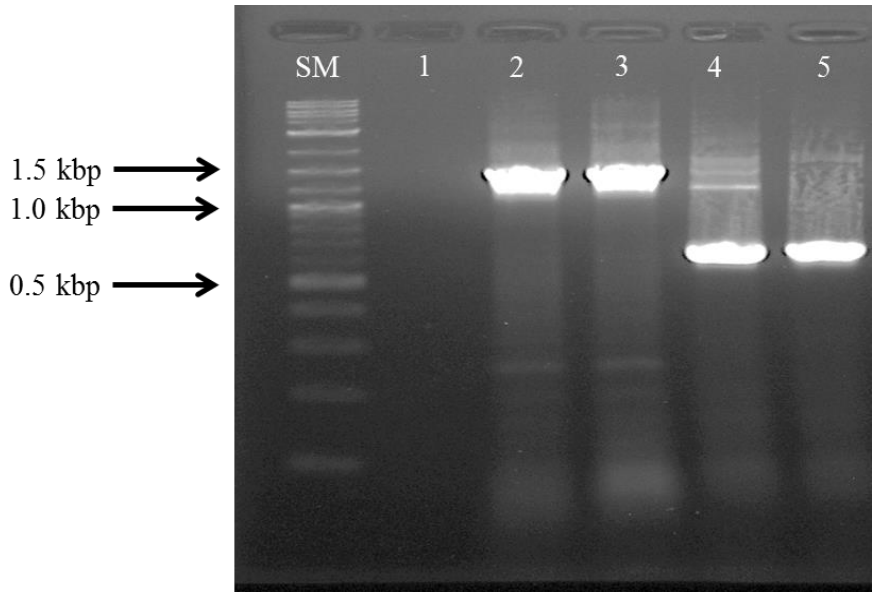

Figure 6. PCR of wild type (Lanes 2 and 3) and Δ*vibF* (Lanes 4 and 5). 2-log ladder is in the lane marked SM and key sizes are indicated by the arrows to the left. All strains were analyzed using primers specific for *vibF*.

A chromosomal mutant of *viuA* was generated by using a previously-constructed plasmid which interrupts the gene sequence with a tetracycline resistant cassette [34]. The strain was shown to be resistant to tetracycline, but to confirm that the mutation was

present PCR with primers *viuA* and the tetracycline cassette was performed. The *viuA* primers amplified 700 base-pairs in the wild type (Figure 7, Lane 2), indicating an intact *viuA* sequence. Amplifying with primers specific to the tetracycline cassette resulted in nonspecific bands, none of which corresponded to the 960 base pair band expected in the presence of the tetracycline cassette amplification (Figure 7, Lane 1). Amplifying *viuA*::*tet*^{R} with primers specific to the tetracycline cassette resulted in a 960 base pair confirming that the tetracycline cassette was present (Figure 7, Lane 3). Amplifying *viuA*::*tet*^{R} with primers specific to *viuA* resulted in a band slightly larger than 1.5 kbp which cooresponded to a 1,660 base pair band showing a successful interruption of *viuA* with the tetracycline cassette (Figure 7, Lane 4).

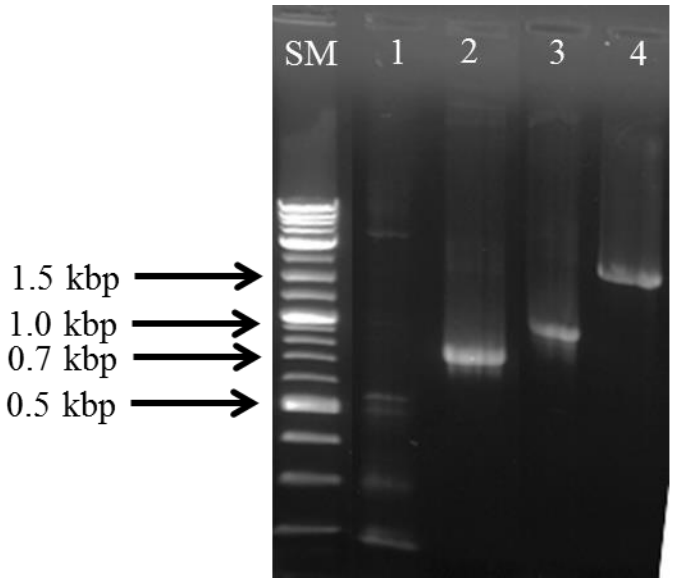

Figure 7. PCR of wild type (Lanes 1 and 2) and *viuA*::*tet*^{R} (Lanes 3 and 4). 2- log ladder is in the lane marked SM and key sizes are indicated. Lanes 1 and 3 were analyzed with internal primers for the tetracycline resistant cassette and lanes 2 and 4 were analyzed with primers flanking *viuA* on the chromosome.

Vibriobactin production of wild type, viuA::tet^R, and ΔvibF

In order to confirm that genetic mutations to *viuA* and *vibF* were affecting vibriobactin production as predicted, *viuA*::*tet*^{R} and Δ*vibF* were assayed for vibriobactin production using chrome azurol S (CAS)-agar plates. The presence of an orange halo and orange hue surrounding the wild type and *viuA*::*tet*^{R} indicate vibriobactin production. Δ*vibF* lacks an orange halo and hue and does not produce vibriobactin (Figure 8).

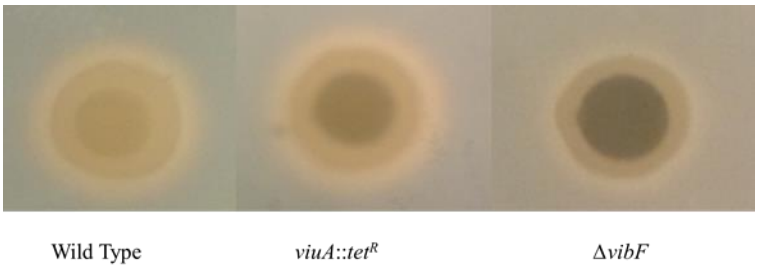

Figure 8. Vibriobactin production analysis of wild type, *viuA*::*tet*^{R}, and Δ*vibF* with chrome azurol S (CAS)-agar. An orange coloration present around the cells indicates vibriobactin production.

This assay confirmed that the deletion of the vibriobactin synthesis gene, *vibF,* resulted in the elimination of vibriobactin production in the mutant. The mutant strain *viuA::tet*^{R}, which was genetically confirmed to contain a tetracycline cassette interruption in the outer membrane vibriobactin receptor gene, *viuA,* was also confirmed to be properly producing vibriobactin.

The inability to synthesize or uptake vibriobactin does not affect the growth rate of the cells

To confirm that mutations to *viuA* or *vibF* did not alter their growth rate I analyzed the growth rate of *viuA*::*tet*^{R} and Δ*vibF* over approximately 9 hours. All strains grew at the same rate in EZRDM and the mutant strains showed no defects compared to the wild type (Figure 9).

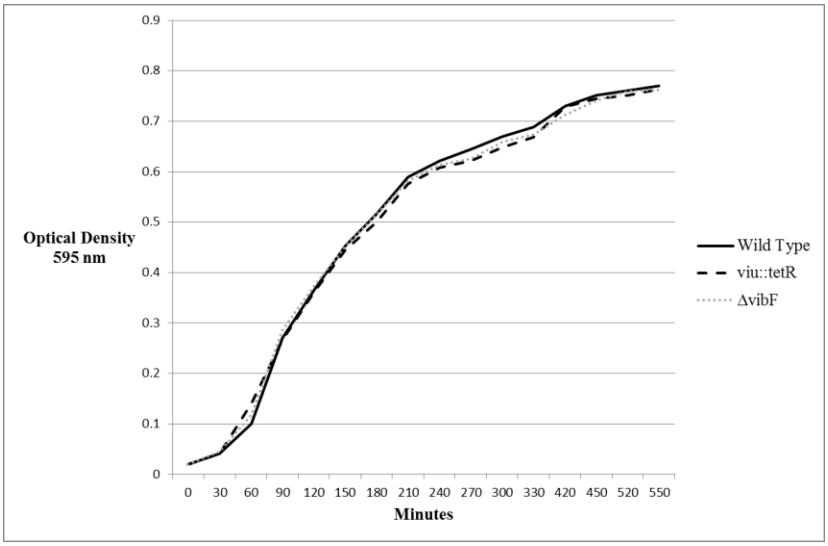

Figure 9. The growth rates of *viuA*::*tet*^{R}, Δ*vibF*, and wild type. The optical density (Y-Axis) represents the cell density of the strains at a given incubation time (X-Axis).

Inability to synthesize or uptake vibriobactin leads to increases in biofilm formation in both iron-replete and –deplete conditions

Since norspermidine has been shown to increase biofilm formation, and is the backbone of vibriobactin, I hypothesized that vibriobactin synthesis and uptake may be important players in biofilm formation. To investigate this hypothesis, I analyzed wild type, *viuA*::*tet*^{R}, and Δ*vibF* for biofilm formation after 24 and 72 hours. The strains were

incubated in EZRDM with or without the addition of 100 µg/ml EDDA. Two way anova analysis showed that both strain type and EDDA treatment had an effect on biofilm formation at both 24 ($p < 0.05$) and 72 ($p < 0.05$) hours (Figure 10).

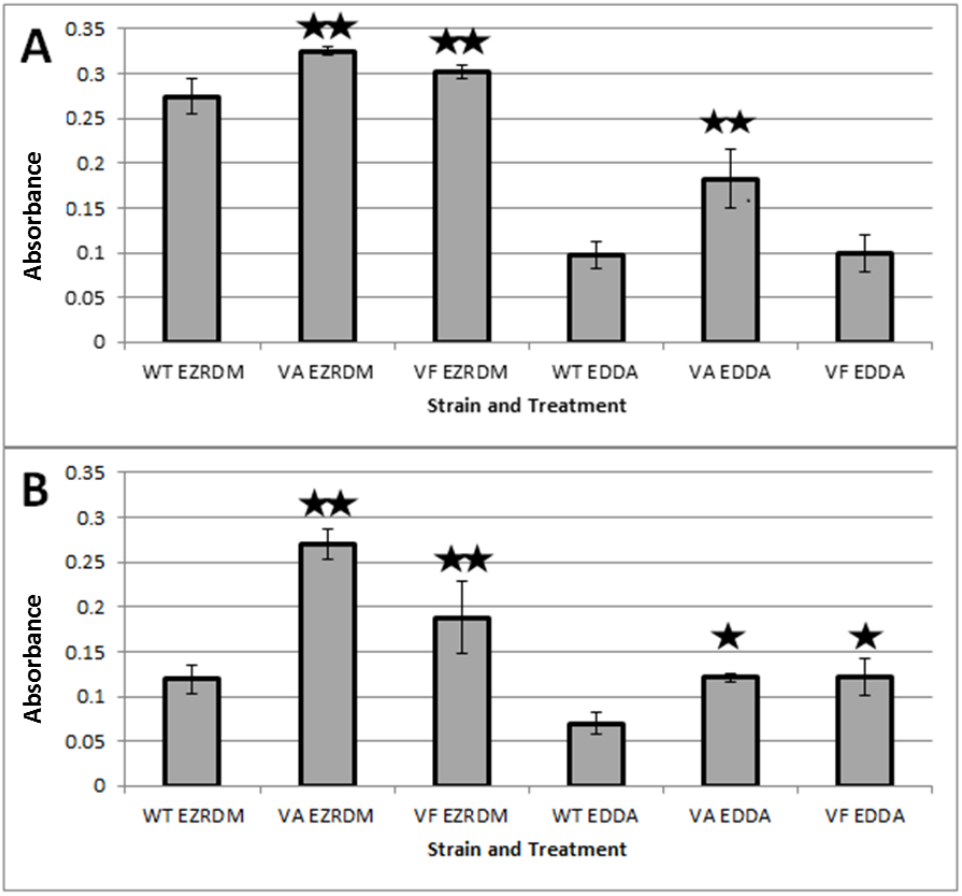

Figure 10. Biofilm formation of wild type (WT), *viuA*::*tet*^{R} (VA), and Δ*vibF* (VF) in iron-replete (EZRDM) or –deplete (EDDA) media after 24 (A) or 72 (B) hours. Absorbance, indicating total biofilm formation, was measured with a spectrophotometer at 595 nm after staining biofilms with 1% crystal violet and is indicated on the Y-axis. Two stars represent statistically significant differences ($p < 0.05$) from the strain of interest and both the wild type and other mutant. Single stars represent a statistically significant difference ($p < 0.05$) from only the wild type.

Each strain was compared to wild type and either Δ*vibF* or *viuA*::*tet*^{R} by Student's T-tests at 24 hours and 72 hours in both iron-replete (EZRDM) and –deplete (EZRDM with 100 µg/ml EDDA) media (Figure 10). Both mutant strains had slightly elevated biofilm formation over the wild type in iron-replete conditions after 24 hours ($p < 0.05$). Interestingly *viuA*::*tet*^{R} also had slightly greater biofilm formation than Δ*vibF* ($p < 0.05$). When treated with 100 µg/ml EDDA there were no discernible differences between wild type and Δ*vibF* after 24 hours. In contrast, biofilm formation by *viuA*::*tet*^{R} was nearly double the amount observed in wild type and Δ*vibF* in iron-deplete media ($p < 0.05$) (Figure 10A).

After 72 hours *viuA*::*tet*^{R} formed approximately 126% more biofilm than wild type in iron-replete media ($p < 0.05$). Δ*vibF* also formed more biofilm than the wild-type by approximately 58% ($p < 0.05$). In iron-replete media *viuA*::*tet*^{R} also formed more biofilm than Δ*vibF* by 75% ($p < 0.05$). In iron-deplete conditions there were no discernible differences between *viuA*::*tet*^{R} and Δ*vibF*, but both mutant strains formed approximately 75% more biofilm than the wild-type ($p < 0.05$) (Figure 10B).

To show that EDDA was not influencing the growth of the different strain and therefore influencing biofilm formation the planktonic cells were quantified as well. After 24 and 72 hours EDDA did not impact the ability of the strains to grown since planktonic cells remained approximately the same across treatments (Figure 11). Planktonic cell numbers were also were not affected by the mutations in EZRDM (data not shown).

Mutations to viuA and vibF result in different abilities to compete with wild type V. cholerae

To determine if mutations to the vibriobactin system gave the mutant strains a competitive advantage for space in a mixed biofilm I investigated how *viuA*::*tet*^{R} and Δ*vibF* interact with wild type cells. To do this I mixed each mutant strain with wild type 1:1 and incubated cultures for 24 and 72 hours in static conditions to facilitate biofilm formation. After either 24 or 72 hours mixed biofilm cells were plated on LB-agar plates containing X-Gal, a lactose analog. On these plates the presence of an intact *lacZ* gene will result in the breakdown of X-Gal resulting in a blue precipitate. Since the wild type used in these experiments has an interrupted *lacZ* gene it remained white, but since the mutant strains have an intact *lacZ* gene they were blue on X-Gal plates. After counting colonies on the plates and comparing the post-incubation biofilm cell ratio to input cell ratios, I was able to calculate competitive indices. Numbers greater than one indicate that the mutant is outcompeting the wild type for space in the biofilm and numbers less than one indicate strains that are being outcompeted by the wild type (Figure 12).

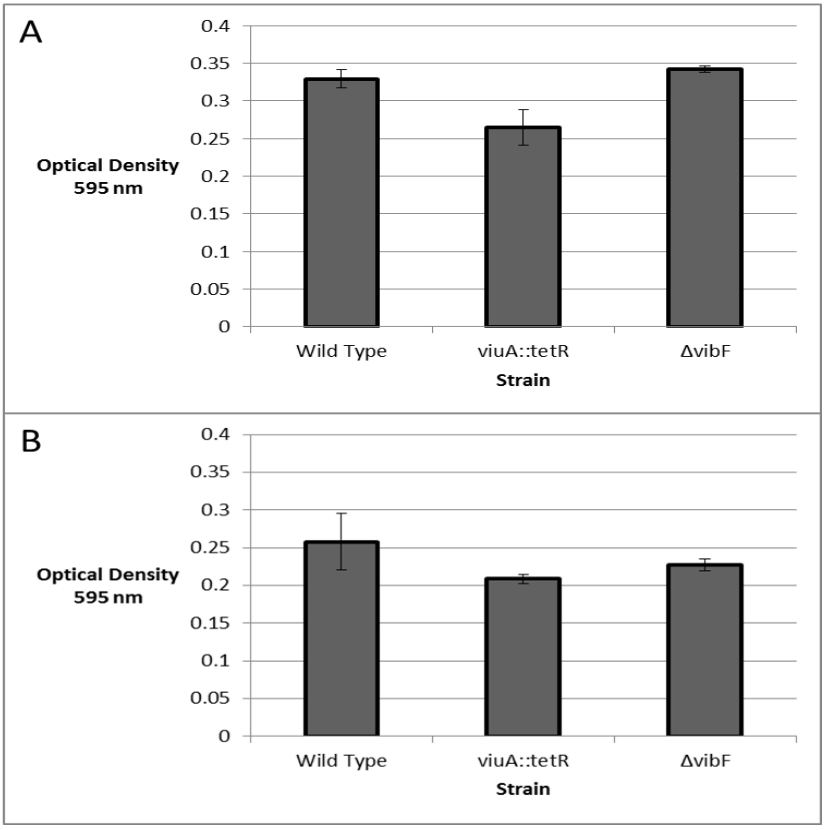

Figure 11. The planktonic growth of wild type, *viuA*::*tet*^{R}, and Δ*vibF* in EZRDM supplemented with 100 µg/ml EDDA. The optical density (Y-Axis) represents the total quantity of cells at an incubation time of 24 (A) or 72 (B) hours.

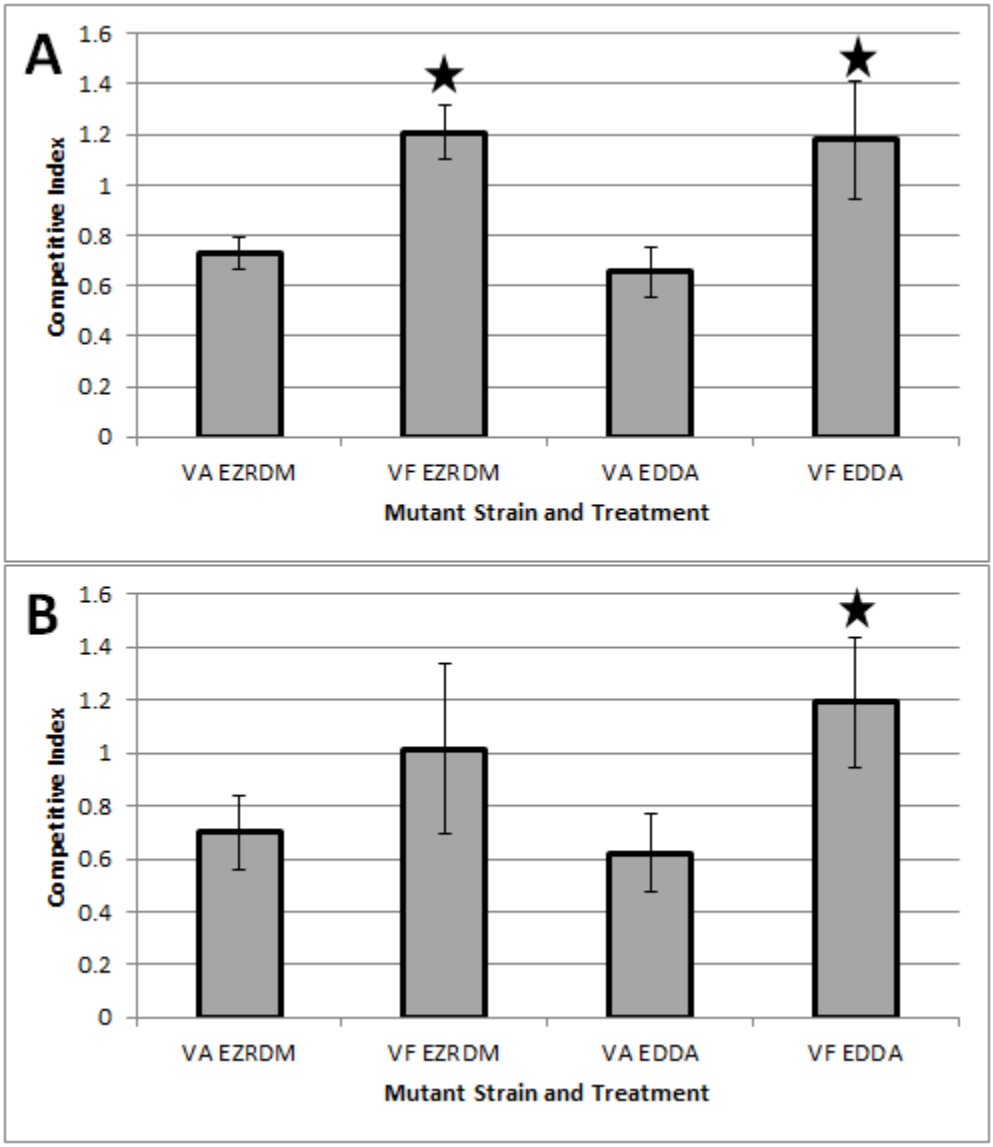

Figure 12. The ability of Δ*vibF* (VF) and *viuA*::*tet*^{R} (VA) to compete with wild type in iron–replete (EZRDM) and –deplete (EDDA) media grown for 24 (A) and 72 (B) hours. Significant differences ($p < 0.05$) between the competitive indices of Δ*vibF* and *viuA*::*tet*^{R} are indicated as single stars.

After 24 hours, Δ*vibF* was shown to be more competitive with the wild-type than *viuA*::*tet*^{R} in both iron-replete and –deplete conditions ($p < 0.05$) and the competitive

indices were unaffected by the addition of the iron chelator EDDA ($p > 0.05$) (Figure 12). After 72 hours there was not a statistically significant difference between the competitive indices of *viuA*::*tet*^{R} and Δ*vibF* in iron-replete conditions ($p > 0.05$), but with the addition of EDDA Δ*vibF* outcompeted the wild-type while *viuA*::*tet*^{R} remained at a competitive disadvantage ($p < 0.05$) (Figure 12B).

Biofilm architecture and maturation is altered by the ability to synthesize or uptake vibriobactin

Biofilm formation is a multistep process involving highly regulated maturation stages. Since mutations to the vibriobactin iron-acquisition system were able to affect biofilm formation we wanted to observe biofilm maturation using confocal laser scanning microscopy (CLSM). Biofilms grown for 24 hours in iron-replete media showed that *viuA*::*tet*^{R} formed thicker biofilms than the wild type with an average thickness of 26.6 µM compared to 15 µM. The Δ*vibF* strain also formed thicker biofilms in comparison to the wild type in iron-replete media with a thickness of 23.3 µM. In iron-deplete media that effect was also apparent with *viuA*::*tet*^{R} which formed biofilms that had an average thickness of 24.33 µM compared to 12.3 µM in the wild-type. The Δ*vibF* strain also formed thicker biofilms than the wild type with an average thickness of 20.66 µM in iron-deplete media (Figure 13).

The biofilm architecture was also observed using confocal microscopy. Both the wild-type and Δ*vibF* formed lawn style biofilms with few microcolonies in iron-replete media (Figure 14 A, E). With the addition of the ferric iron chelator EDDA some early

microcolonies were visible in Δ*vibF* but it still closely resembled the lawn style biofilm characteristic of the wild-type after 24 hours (Figure 14 B, F).

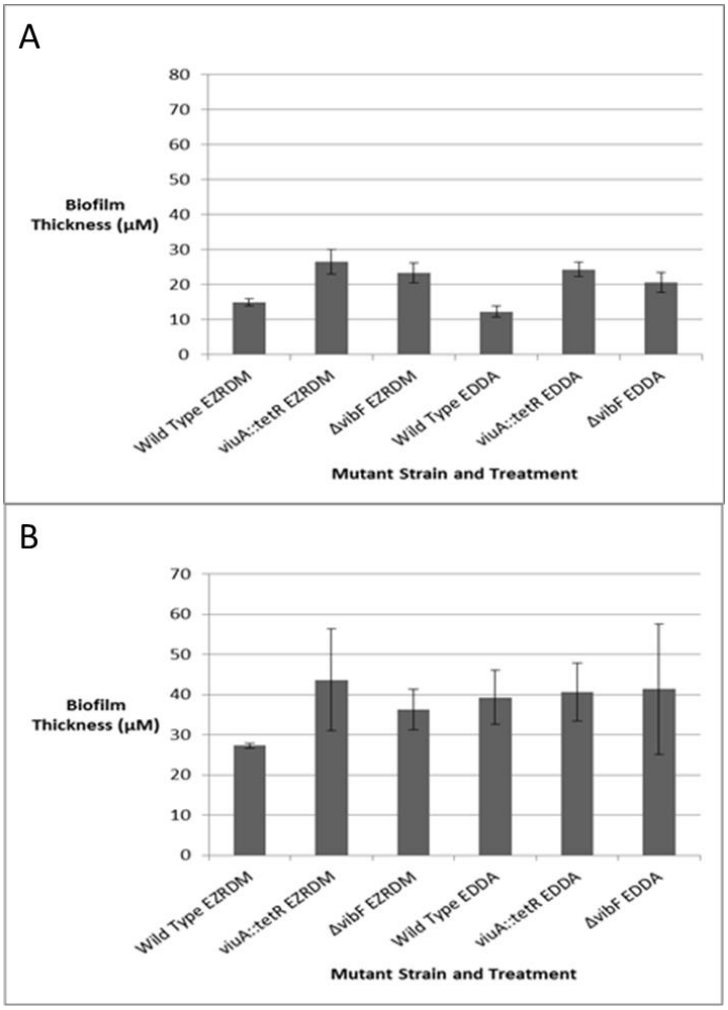

Figure 13. Biofilm thickness of wild type, *viuA*::*tet*^{R}, and Δ*vibF* after 24 hours (A) and 72 hours (B) in iron-replete (EZRDM) or –deplete (EDDA) media analyzed by confocal laser scanning microscopy (CLSM) with SYTO-9. Thickness is measured in µM and is indicated on the Y-Axis and each strain and treatment is indicated on the X-Axis.

The *viuA*::*tet*^{R} mutant formed biofilms vastly different than those observed in the wild-type after 24 hours. In both iron-replete and –deplete conditions *viuA*::*tet*^{R} formed much more densely packed biofilms with apparent microcolonies (Figure 14 C, D). The thick microcolonies were separated by prevalent channels. In both Δ*vibF* and the wild-type these channels were not as pronounced as they are in *viuA*::*tet*^{R} (Figure 14 A, B, E, F).

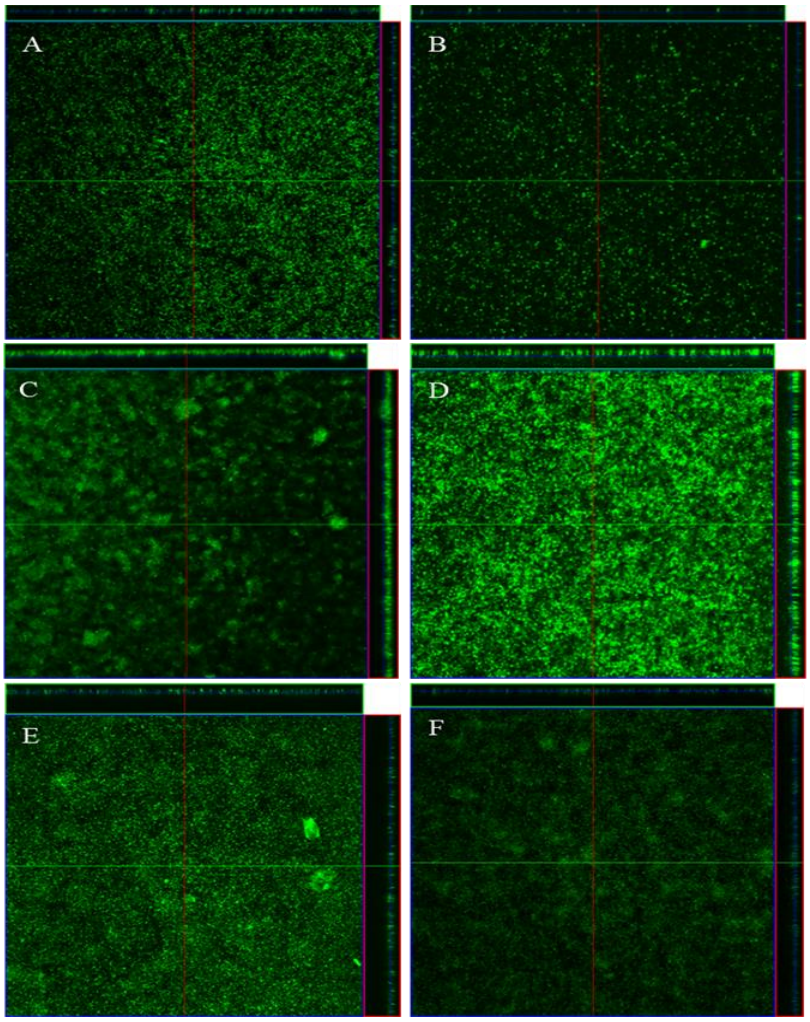

Figure 14. Biofilm formation of wild type (A and B), viuA::tetR (C and D), and ΔvibF (E and F)after 24 hours in iron-replete (A, C, and E) or –deplete (B, D, and F) media analyzed by confocal laser scanning microscopy (CLSM) with SYTO-9. CLSM images were taken at 20x and the z-stacks on the top and right of the image indicate a cross-section of the biofilm. In each panel the field of view represents a top-down view of the biofilm and the z-stacks on the top and right of the image indicate a cross-section of the biofilm. The top z-stack represents a cross section along the vertical line through the top down image and the right z-stack indicates a cross-section along the horizontal line.

Biofilms grown for 72 hours in iron-rich and –deplete media were also examined with CLSM to observe biofilm maturation and microcolony formation in later stage biofilms. Interestingly, both *viuA*::*tet*^{R} and Δ*vibF* formed much thicker biofilms in iron-replete media with average thicknesses of 43.67 μM and 36.33 μM respectively compared to an average thickness of 27.33 μM in the wild type. Wild type, *viuA*::*tet*^{R}, and Δ*vibF* all formed biofilms with similar thicknesses of 39.3, 43.67, and 41.3 μM respectively (Figure 13B).

Biofilm microcolony formation was also effected by the ability to synthesize or uptake vibriobactin in our mutant strains after 72 hours. The wild type began to form microcolonies as expected after 72 hours in both iron-replete and –deplete media (Figure 15 A, B). In iron-replete media both wild type and Δ*vibF* formed very comparable biofilms with small microcolonies and many easily identifiable channels (Figure 15 A, E). On the other hand *viuA*::*tet*^{R} formed tightly packed and thick microcolonies with thin channels through the biofilm (Figure 15 C). In iron-deplete media both the wild type and *viuA*::*tet*^{R} formed small microcolonies that were interspersed with channels (Figure 15 B, D). When treated with EDDA Δ*vibF* formed very numerous and very large mushroom style microcolonies that spanned up to 75 μM from the surface in the most extreme cases (Figure 15 F). These microcolonies were interspersed with far fewer channels than the other two strains on average.

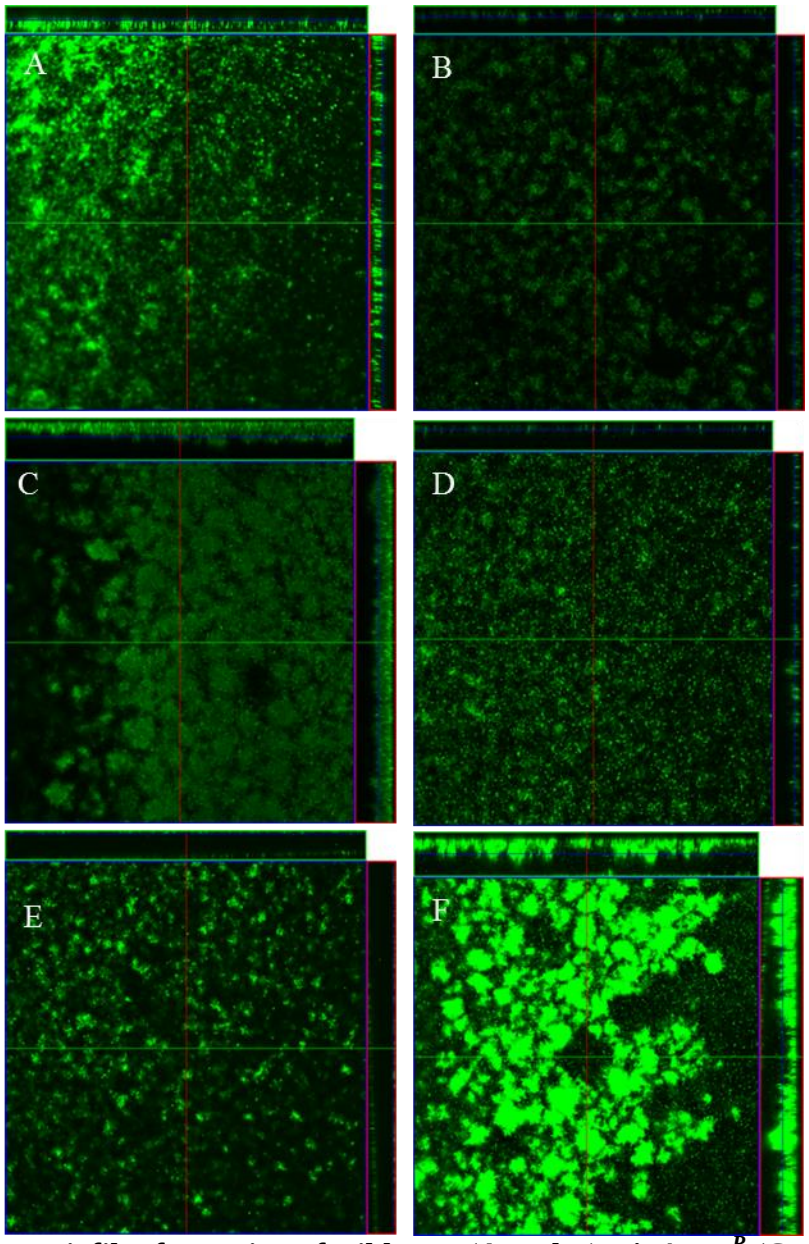

Figure 15. Biofilm formation of wild type (A and B), *viuA*::*tet*^{R} (C and D), and Δ*vibF* (E and F) after 72 hours in iron-replete (A, C, and E) or –deplete (B, D, and F) media analyzed by confocal laser scanning microscopy (CLSM) with SYTO-9. CLSM images were taken at 20x. In each panel the field of view represents a top-down view of the biofilm and the z-stacks on the top and right of the image indicate a cross-section of the biofilm. The top z-stack represents a cross section along the vertical line through the top down image and the right z-stack indicates a cross-section along the horizontal line.

Mutations to vibriobactin synthesis or uptake have modified spatial arrangement in biofilms when mixed with wild type

To analyze the distribution of cells competing for space in mixed biofilms the mutant strains were transformed with a plasmid encoding mCherry, a red fluorescent protein, and the wild type was transformed with a plasmid encoding green fluorescent protein (GFP). After inoculating EZRDM or EZRDM with 100 µg/ml EDDA 1:1 with wild type and either *viuA*::*tet*^{R} or Δ*vibF* the cultures were incubated for 24 or 72 hours in static conditions so that they formed a biofilm on a glass cover slip. The biofilm was then analyzed using CLSM.

After 24 hours the phenotypic trend was the same in both mutants and in both iron-replete and –deplete conditions. The mutant strains formed lawn-style biofilms that covered nearly the entire surface of the field of view and had few channels. The wild type did not form a lawn style biofilm with complete coverage. Instead, it formed biofilm structures with many channels and small microcolonies. Neither wild type nor the mutant strains formed microcolonies after 24 hours that projected far outward from the surface (Figures 16 and 17).

Biofilms were also analyzed after 72 hours in both iron-replete and –deplete media. In iron-replete media biofilms were thicker but the phenotypes were similar to those observed after 24 hours. The mutant strains formed a lawn style biofilm with nearly complete coverage of the field of view. The wild type again formed almost exclusively as

microcolonies with numerous channels. Interestingly thick microcolonies projected out from the base of the surface and included both mutant and wild type cells (Figure 18).

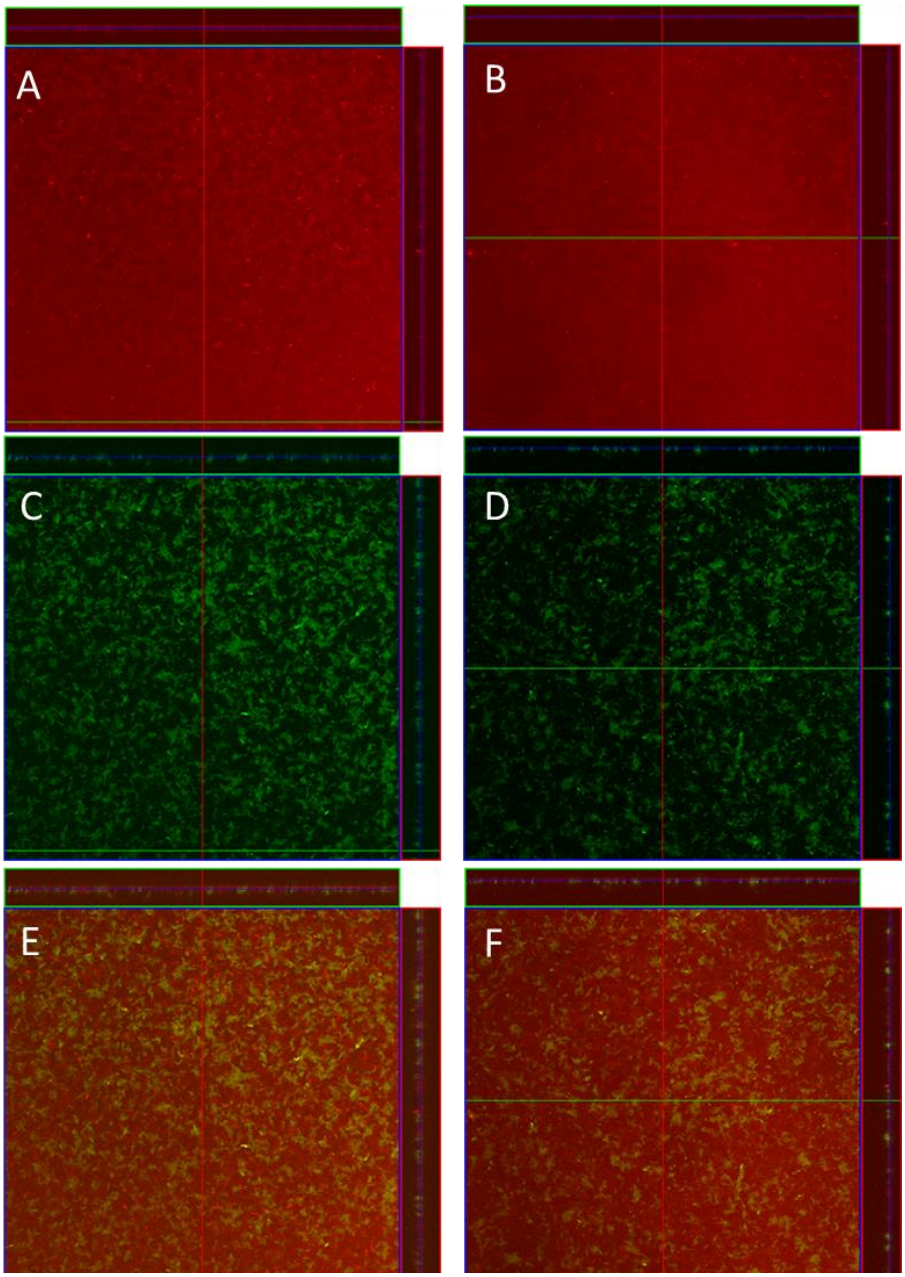

Figure 16. CLSM images of wild type (GFP)(C and D) incubated equally for 24 hours in EZRDM with either *viuA*::*tet*^{R} (mCherry)(A) or Δ*vibF* (mCherry)(B). The merge is both the mutant strain and wild type layered together (E and F). CLSM images were taken at 20x. In each panel the field of view represents a top-down view of the biofilm and the z-stacks on the top and right of the image indicate a cross-section of the biofilm. The top z-stack represents a cross section along the vertical line through the top down image and the right z-stack indicates a cross-section along the horizontal line.

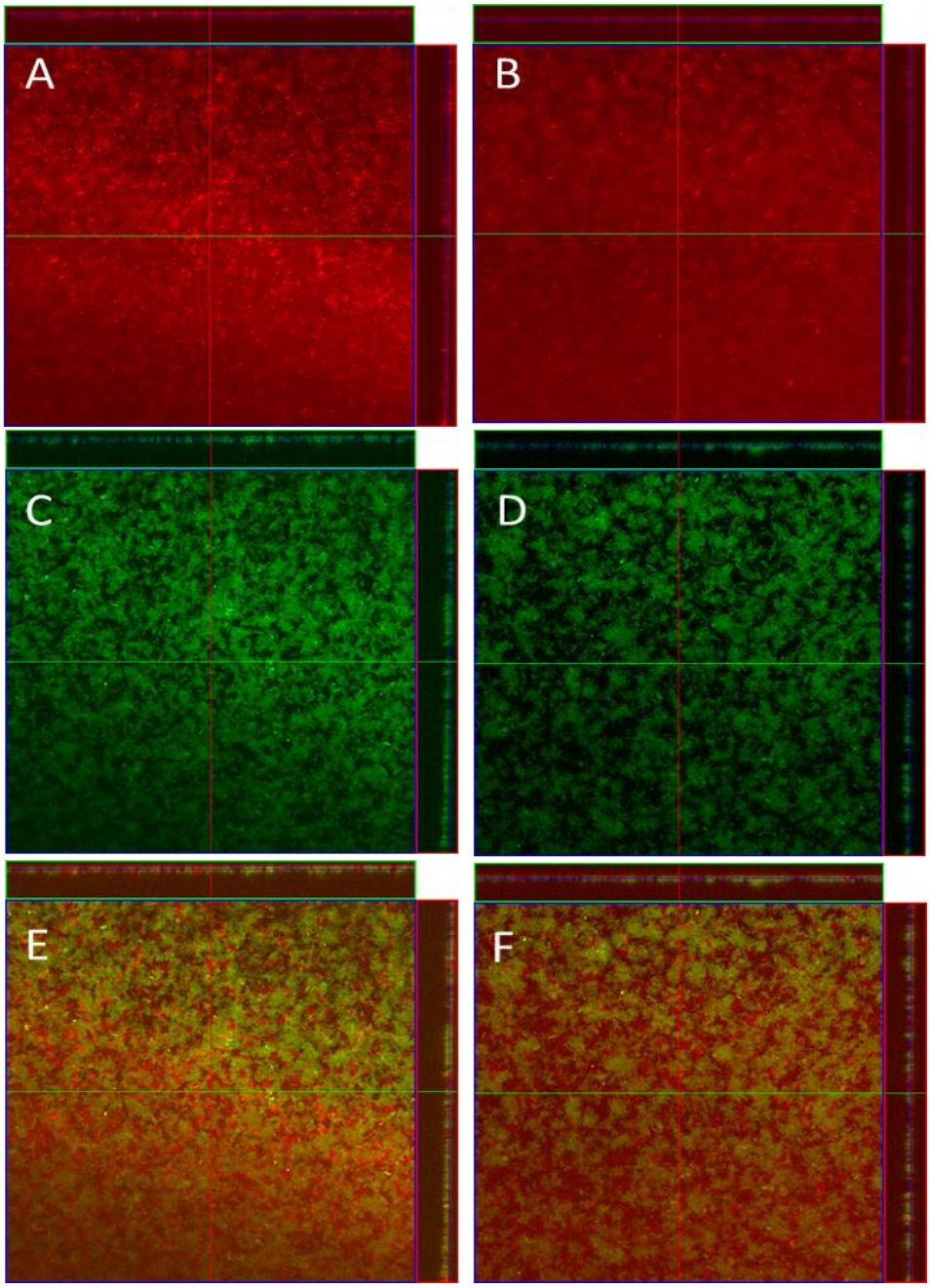

Figure 17. CLSM images of wild type (GFP)(C and D) incubated equally with either *viuA*::*tet*^{R} (mCherry)(A) or Δ*vibF* (mCherry)(B) for 24 hours in EZRDM with 100 µg/ml EDDA. The merge is both the mutant strain and wild type layered together (E and F). CLSM images were taken at 20x. In each panel the field of view represents a top-down view of the biofilm and the z-stacks on the top and right of the image indicate a cross-section of the biofilm. The top z-stack represents a cross section along the vertical line through the top down image and the right z-stack indicates a cross-section along the horizontal line.

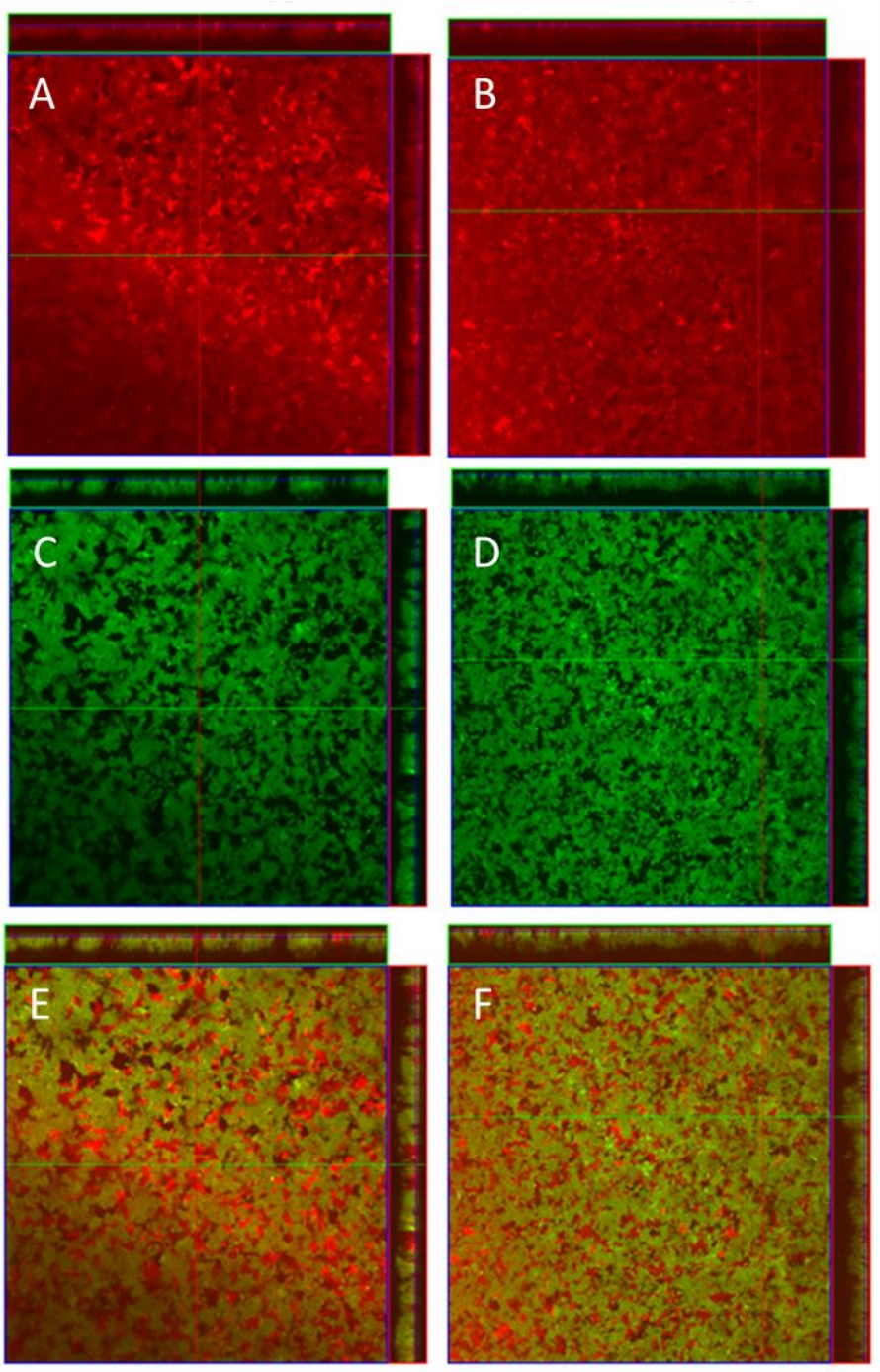

Figure 18. CLSM images of wild type (GFP)(C and D) incubated equally for 72 hours in EZRDM with either *viuA*::*tet*^{R} (mCherry)(A) or Δ*vibF* (mCherry)(B). The merge is both the mutant strain and wild type layered together (E and F). CLSM images were taken at 20x. In each panel the field of view represents a top-down view of the biofilm and the z-stacks on the top and right of the image indicate a cross-section of the biofilm. The top z-stack represents a cross section along the vertical line through the top down image and the right z-stack indicates a cross-section along the horizontal line.

In iron-deplete conditions after 72 hours the phenotype of *viuA*::*tet*^{R} mixed with wild type was similar to all other time points and conditions. The *viuA*::*tet*^{R} mutant formed the characteristic lawn style biofilm and the wild type formed primarily as microcolonies. Δ*vibF* formed primarily microcolonies with many channels and mixed well with wild type microcolonies. The wild type again formed consistently to previous time points and conditions (Figure 19).

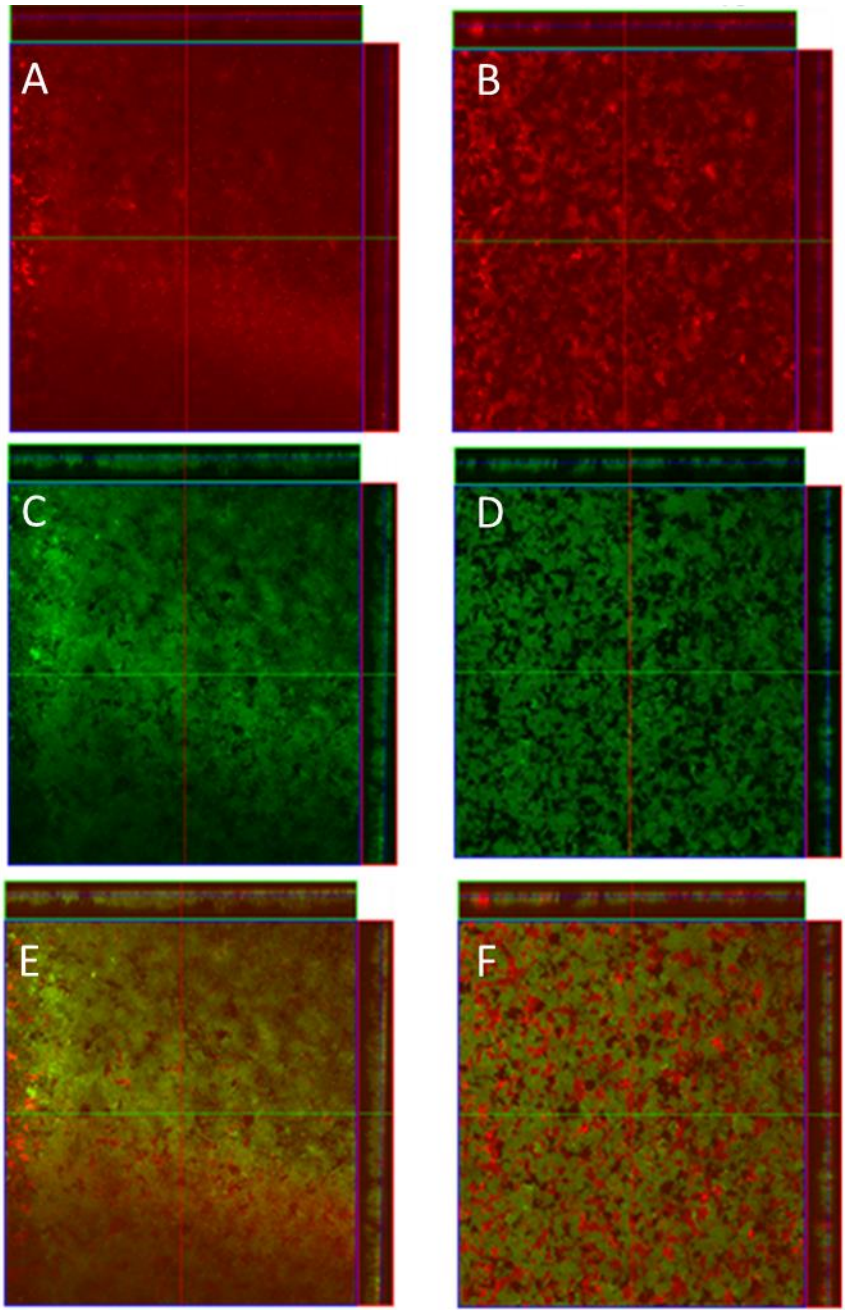

Figure 19. CLSM images of wild type (GFP)(C and D) incubated equally with either viuA::tetR (mCherry)(A) or ΔvibF (mCherry)(B) for 72 hours in EZRDM with 100 µg/ml EDDA. The merge is both the mutant strain and wild type layered together (E and F). CLSM images were taken at 20x. In each panel the field of view represents a top-down view of the biofilm and the z-stacks on the top and right of the image indicate a cross-section of the biofilm. The top z-stack represents a cross section along the vertical line through the top down image and the right z-stack indicates a cross-section along the horizontal line

Discussion

This study aimed to 1) investigate whether biofilm cell quantity was affected by iron levels and the ability to synthesize and use vibriobactin; 2) examine the role of vibriobactin and iron level on biofilm maturation and architecture; and 3) investigate whether the lack of vibriobactin synthesis or uptake provides *V. cholerae* with any competitive differences when mixed with wild type. I have shown that vibriobactin and iron levels do affect biofilm formation in *V. cholerae*. Vibriobactin deficient mutants showed increased biofilm formation in both iron-replete and –deplete conditions. In addition, results showing that wild-type *V. cholerae* MO10 biofilm formation is reduced in iron-deplete conditions closely mirroring that shown in wild type *V. cholerae* El Tor [26]. Competitive indices were also calculated and indicated that Δ*vibF* was able to outcompete the wild type for space in biofilms, but that *viuA*::*tet*^{R} was outcompeted for space in biofilms by the wild type.

I hypothesized that vibriobactin and free iron levels were important for biofilm formation since norspermidine, a polyamine that upregulates biofilm formation, acts as the backbone for vibriobactin [21]. After constructing mutants defective in vibriobactin uptake, *viuA*::*tet*^{R}, and synthesis, Δ*vibF*, biofilm formation was compared to that of wild-type *V. cholerae*. Since vibriobactin synthesis genes are upregulated when iron is in low supply *viuA* and *vibF* are only relevant for iron acquisition in iron-deplete conditions.

Biofilm formation was increased after 24 hours in both mutants in iron-replete conditions, albeit only slightly. This effect was much more pronounced in *viuA*::*tet*^{R} in

iron-deplete conditions where it formed twice as much biofilm compared to the wild type and Δ*vibF*, which were indistinguishable. After 72 hours, the increase in biofilm cells of both *viuA*::*tet*^{R} and Δ*vibF* were more than double the wild type in both iron-replete and –deplete conditions.

It is likely that the effect of the inability to synthesize or uptake vibriobactin was more pronounced after 72 hours for a number of reasons. First, since all biofilms were inoculated from bacteria grown overnight in EZRDM without chelator all strains had an initial store of iron at the start of the biofilm assay. As these internal stores become depleted it is likely that the effects of vibriobactin mutations became more apparent. The second possible reason for increased biofilm formation in the mutant strains may be tied to an increase in norspermidine.

Since norspermidine is necessary for the formation of vibriobactin, the mutation of the vibriobactin system may lead to an increase in cellular norspermidine concentrations leading to an increase in biofilm formation. This may be occurring in two different ways depending on the mutant strain. The first strain, *viuA*::*tet*^{R}, maintains the ability to produce vibriobactin, but since the outer membrane receptor is disrupted it cannot import the molecule. Since *viuA*::*tet*^{R} cells are not importing vibriobactin the environment appears to be iron limited from the perspective of the cell. This then leads to increased and continuing production of vibriobactin, which in turn may lead to an increase in norspermidine production to provide the materials for vibriobactin synthesis. In the second mutant strain, Δ*vibF*, increased biofilm formation may also be linked to

norspermidine. Since VibF is responsible for binding oxazoline rings to norspermidine the deletion of the gene encoding this enzyme means that norspermidine cannot be used to make vibriobactin; therefore, the internal norspermidine concentration may be increased [18].

As biofilms mature, cells in the biofilm die and lyse. As this process occurs the contents of dead cells are released into the environment and can be utilized by the living cells remaining in the biofilm. In this case dead mutant cells would release their internal supplies of norspermidine. Since internal norspermidine levels may be elevated in the mutant strains this would result in a greater amount of biofilm enhancing signal over time compared to the wild type. Furthermore, since the possibility of norspermidine increasing within the cell happens over time this may explain why the effects of increased biofilm formation are more apparent after 72 hours. Preliminary high pressure liquid chromatography experiments quantifying intracellular polyamines have shown that norspermidine levels are higher in both *viuA*::tet^R and Δ*vibF* (data not shown).

A second hypothesis for increased biofilm formation in *viuA*::tet^R and Δ*vibF* is that due to iron starvation the production of biofilm structures may be favored. The reason is that exopolysaccharide (EPS), which is a key component of biofilm formation and maturation, is a powerful iron binding compound in a variety of bacteria [37,38,39,40,41]. In *P. aeruginosa* it has been suggested the EPS provides carboxyl sites which act to bind iron and other metal ions [41]. *P. aeruginosa* biofilms have also been shown to contain more ferrous iron than planktonic cells. This was likely a result of the

reduction of ferric iron to ferrous iron during metabolism [40]. As dying cells lyse they release their internal nutrient stores and EPS can trap ferrous iron, making it available to the surrounding cells. Other bacteria have also been shown to use EPS to trap metal ions and iron or to survive iron-stress including *Klebsiella oxytoca*, *Vibrio anguillarum*, *Bradyrhizobium japonicus*, and *Paracoccus zeaxanthinifaciens* [38,42,43,44].

The hypothesis that the use of EPS as an iron trap may be driving biofilm formation in *viuA*::*tet*^{R} and Δ*vibF* is partially supported by the confocal images showing greater microcolony formation in *viuA*::*tet*^{R} and Δ*vibF*. EPS is necessary for late stage biofilms and biofilm maturation into mushroom style microcolonies. Since ferric and ferrous iron can be trapped by EPS it may be a way for cells to prevent iron from lysed cells diffusing into the environment and being trapped by EDDA. To investigate this hypothesis more thoroughly it will be necessary to analyze *vibrio polysaccharide* (*vps*) genes to see if they are upregulated and if more VPS is being produced. This can also be visualized using scanning electron microscopy (SEM), which also provides the tools necessary to analyze the level of iron within microcolonies. When electrons are used to generate an image with SEM they generate X-Rays. Each element produces a characteristic X-Ray pattern that can be collected using a specialized detector. This technique, called Wavelength Dispersive X-Ray Spectroscopy (WDS), generates an elemental map that indicates the location of different elements and their levels. These assays are currently in progress in the Karatan lab.

Since *viuA*::*tet*^{R} and Δ*vibF* formed drastically different amounts of biofilms and structures I wanted to examine how they would compete with the wild type in mixed cultures. The first goal of the competition experiments was to see if the loss of uptake of vibriobactin or the loss of vibriobactin synthesis impacted the ability to exist in biofilms with wild type. The second was to determine if the presence of external vibriobactin, supplied by the wild type, reduced the amount of biofilm cells in the mutants. Lastly, it was important to see how *viuA*::*tet*^{R} and Δ*vibF* may interact in mixed culture since bacteria are commonly found as part of mixed microbiota in a host organism or in aquatic environments.

First, quantitative experiments were performed on X-Gal plates where wild type cells appeared blue and mutant cells appeared white. At both 24 and 72 hours in iron-rich and –deplete media *viuA*::*tet*^{R} was outcompeted by the wild type and Δ*vibF* outcompeted the wild type. The ability of Δ*vibF* to outcompete the wild type may have been due to more available growth resources necessary to produce biofilm structures. Since Δ*vibF* still had the ability to uptake vibriobactin produced by the wild type it likely had more resources available produce extra biofilm structures.

The *viuA*::*tet*^{R} mutant was outcompeted by the wild type for space in the biofilm. It is also a possibility that this effect is due to energy dynamics since *viuA*::*tet*^{R} cells would be producing vibriobactin at a high rate due to their perception of exceptionally iron-limited media. Interestingly though *viuA*::*tet*^{R} formed the most biofilm in monoculture biofilm assays. It is possible that wild type was utilizing siderophores

produced by the *viuA*::*tet*^{R} mutant to focus on producing biofilm structures, very much the opposite of what is happening in competition with Δ*vibF*. To test these hypotheses gene expression or vibriobactin analysis assays will need to be performed to determine the level of vibriobactin production in wild type, *viuA*::*tet*^{R}, and Δ*vibF*.

Confocal microscopy was also utilized to analyze how *viuA*::*tet*^{R} and Δ*vibF* interact in mixed cultures with wild type. Both mutant strains, *viuA*::*tet*^{R} and Δ*vibF*, were transformed with a plasmid encoding mCherry and wild type was transformed with a plasmid encoding GFP. Although competitive indices were drastically different in the quantitative experiments the two mutants had nearly identical biofilm distributions when mixed with wild type. At both time points and in both iron-replete and -deplete environments the mutants formed a biofilm with nearly complete surface coverage and thick microcolonies. The wild type on the other hand existed almost exclusively in thick microcolonies at both time points and conditions.

This distribution is interesting considering that the mutants seem to favor a lawn style biofilm with large surface coverage while the wild type forms almost exclusively microcolonies with many channels. Although the mutants form lawn style biofilms they also are included in many of the wild type microcolonies as well. This may again be indicative of exopolysaccharide being used to trap iron since vibriobactin is present in the mixed biofilms. It could also be that mutant cells are receiving a signal to form normal microcolonies with the wild type, but also having areas where coverage without channels is still present due to the same signals present in monoculture biofilms. The Δ*vibF* mutant

does seem to return to the wild type style biofilm after 72 hours in EDDA, which may be due to its use of wild type synthesized vibriobactin. The restoration of biofilm phenotypes when siderophores are added to *P. aeruginosa* mutants defective in siderophore production has been shown previously [22]. There is also evidence that supplying iron-starved *E. coli* with chelated iron restores biofilm phenotypes [23].

The link between iron availability, siderophore use, and biofilm formation is especially important considering recent developments in treating antibiotic resistant bacteria with iron chelators to remove infections [45,46,47,48,49]. Since biofilms have been shown to be resistant to antibiotics, and may be a way of persisting in the human host, understanding how iron and biofilms are linked is crucial to investigating the possible problems or complications with these chelation based therapies. Furthermore, the role of siderophores in biofilm formation has been primarily studied in *P. aeruginosa.* Since virtually all iron-uptake systems in *V. cholerae* are identified the use of it as a model system for understanding to role of iron in biofilm formation of Gram-negative bacteria is very promising Although mechanistic studies must be performed to discover the specific role that iron and vibriobactin play in biofilm formation this work strongly suggests that both are influential in biofilm formation and maturation.

References

1. Wyckoff EE, Payne SM (2011) The *Vibrio cholerae VctPDGC* system transports catechol siderophores and a siderophore-free iron ligand. Mol Microbiol 81: 1446-1458.
2. Andrews SC, Robinson AK, Rodriguez-Quinones F (2003) Bacterial iron homeostasis. FEMS Microbiol Rev 27: 215-237.
3. Touati D (2000) Iron and oxidative stress in bacteria. Arch Biochem Biophys 373: 1-6.
4. Doherty CP (2007) Host-pathogen interactions: the role of iron. J Nutr 137: 1341-1344.
5. Neilands JB (1995) Siderophores: structure and function of microbial iron transport compounds. J Biol Chem 270: 26723-26726.
6. Haselwandter K, Haninger G, Ganzera M (2011) Hydroxamate siderophores of the ectomycorrhizal fungi Suillus granulatus and S. luteus. Biometals 24: 153-157.
7. Keberle H (1964) The biochemistry of desferrioxamine and its relation to iron metabolism. Ann N Y Acad Sci 119: 758-768.
8. Wyckoff EE, Valle AM, Smith SL, Payne SM (1999) A multifunctional ATP-binding cassette transporter system from Vibrio cholerae transports vibriobactin and enterobactin. J Bacteriol 181: 7588-7596.
9. Budzikiewicz H (1993) Secondary metabolites from fluorescent pseudomonads. FEMS Microbiol Rev 10: 209-228.

10. Farnaud S, Evans RW (2003) Lactoferrin--a multifunctional protein with antimicrobial properties. Mol Immunol 40: 395-405.

11. Schaible UE, Kaufmann SH (2004) Iron and microbial infection. Nat Rev Microbiol 2: 946-953.

12. Cornelis P, Matthijs S, Van Oeffelen L (2009) Iron uptake regulation in *Pseudomonas aeruginosa*. Biometals 22: 15-22.

13. Matzanke BF, Bohnke R, Mollmann U, Reissbrodt R, Schunemann V, et al. (1997) Iron uptake and intracellular metal transfer in mycobacteria mediated by xenosiderophores. Biometals 10: 193-203.

14. Strange HR, Zola TA, Cornelissen CN (2011) The fbpABC operon is required for Ton-independent utilization of xenosiderophores by *Neisseria gonorrhoeae* strain FA19. Infect Immun 79: 267-278.

15. Wyckoff EE, Mey AR, Payne SM (2007) Iron acquisition in *Vibrio cholerae*. Biometals 20: 405-416.

16. Chu BC, Garcia-Herrero A, Johanson TH, Krewulak KD, Lau CK, et al. (2010) Siderophore uptake in bacteria and the battle for iron with the host; a bird's eye view. Biometals 23: 601-611.

17. Mey AR, Wyckoff EE, Kanukurthy V, Fisher CR, Payne SM (2005) Iron and fur regulation in *Vibrio cholerae* and the role of fur in virulence. Infect Immun 73: 8167-8178.

18. Crosa JH, Walsh CT (2002) Genetics and assembly line enzymology of siderophore biosynthesis in bacteria. Microbiol Mol Biol Rev 66: 223-249.

19. Zhu J, Mekalanos JJ (2003) Quorum sensing-dependent biofilms enhance colonization in *Vibrio cholerae*. Dev Cell 5: 647-656.

20. Faruque SM, Biswas K, Udden SM, Ahmad QS, Sack DA, et al. (2006) Transmissibility of cholera: in vivo-formed biofilms and their relationship to infectivity and persistence in the environment. Proc Natl Acad Sci U S A 103: 6350-6355.

21. Karatan E, Duncan TR, Watnick PI (2005) NspS, a predicted polyamine sensor, mediates activation of *Vibrio cholerae* biofilm formation by norspermidine. J Bacteriol 187: 7434-7443.

22. Banin A (2005) Planetary science. The enigma of the martian soil. Science 309: 888-890.

23. Wu Y, Outten FW (2009) IscR controls iron-dependent biofilm formation in *Escherichia coli* by regulating type I fimbria expression. J Bacteriol 191: 1248-1257.

24. Johnson M, Cockayne A, Williams PH, Morrissey JA (2005) Iron-responsive regulation of biofilm formation in staphylococcus aureus involves fur-dependent and fur-independent mechanisms. J Bacteriol 187: 8211-8215.

25. Ojha A, Hatfull GF (2007) The role of iron in *Mycobacterium smegmatis* biofilm formation: the exochelin siderophore is essential in limiting iron conditions for biofilm formation but not for planktonic growth. Mol Microbiol 66: 468-483.

26. Mey AR, Craig SA, Payne SM (2005) Characterization of *Vibrio cholerae* RyhB: the RyhB regulon and role of ryhB in biofilm formation. Infect Immun 73: 5706-5719.

27. Miller VL, Mekalanos JJ (1988) A novel suicide vector and its use in construction of insertion mutations - osmoregulation of outer-membrane proteins and virulence determinants in *Vibrio cholerae* requires ToxR. J Bacteriol 170: 2575-2583.

28. Haugo AJ, Watnick PI (2002) *Vibrio cholerae* CytR is a repressor of biofilm development. Mol Microbiol 45: 471-483.

29. Waldor MK, Mekalanos JJ (1994) Emergence of a new cholera pandemic - molecular analysis of virulence determinants in *Vibrio cholerae* O139 and development of a live vaccine prototype. Journal of Infectious Diseases 170: 278-283.

30. Daly C (2013) Zebrafish as a model organism for *Vibrio cholerae* infection. Senior Thesis: Appalachian State University, Boone, NC.

31. Bloemberg GV, OToole GA, Lugtenberg BJJ, Kolter R (1997) Green fluorescent protein as a marker for Pseudomonas spp. Appl Environ Microbiol 63: 4543-4551.

32. Irie Y, Borlee BR, O'Connor JR, Hill PJ, Harwood CS, et al. (2012) Self-produced exopolysaccharide is a signal that stimulates biofilm formation in Pseudomonas aeruginosa. Proc Natl Acad Sci U S A 109: 20632-20636.

33. Butterton JR, Choi MH, Watnick PI, Carroll PA, Calderwood SB (2000) *Vibrio cholerae* VibF is required for vibriobactin synthesis and is a member of the family of nonribosomal peptide synthetases. J Bacteriol 182: 1731-1738.

34. Tashima KT, Carroll PA, Rogers MB, Calderwood SB (1996) Relative importance of three iron-regulated outer membrane proteins for in vivo growth of Vibrio cholerae. Infect Immun 64: 1756-1761.

35. Rogers HJ (1973) Iron-Binding Catechols and Virulence in Escherichia coli. Infect Immun 7: 445-456.

36. Louden BC, Haarmann D, Lynne AM (2011) Use of blue agar CAS assay for siderophore detection. J Microbiol Biol Educ 12: 51-53.

37. Moppert X, Le Costaouec T, Raguenes G, Courtois A, Simon-Colin C, et al. (2009) Investigations into the uptake of copper, iron and selenium by a highly sulphated bacterial exopolysaccharide isolated from microbial mats. J Ind Microbiol Biotechnol 36: 599-604.

38. Leone S, De Castro C, Parrilli M, Baldi F, Lanzetta R (2007) Structure of the iron-binding exopolysaccharide produced anaerobically by the gram-negative bacterium *Klebsiella oxytoca* BAS-10. European Journal of Organic Chemistry: 5183-5189.

39. Baldi F, Marchetto D, Battistel D, Daniele S, Faleri C, et al. (2009) Iron-binding characterization and polysaccharide production by *Klebsiella oxytoca* strain isolated from mine acid drainage. J Appl Microbiol 107: 1241-1250.

40. Lee JU, Beveridge TJ (2001) Interaction between iron and *Pseudomonas aeruginosa* biofilms attached to Sepharose surfaces. Chemical Geology 180: 67-80.

41. Langley S, Beveridge TJ (1999) Metal binding by *Pseudomonas aeruginosa* PAO1 is influenced by growth of the cells as a biofilm. Can J Microbiol 45: 616-622.

42. Croxatto A, Lauritz J, Chen C, Milton DL (2007) *Vibrio anguillarum* colonization of rainbow trout integument requires a DNA locus involved in exopolysaccharide transport and biosynthesis. Environ Microbiol 9: 370-382.

43. Weber B, Chen C, Milton DL (2010) Colonization of fish skin is vital for *Vibrio anguillarum* to cause disease. Environ Microbiol Rep 2: 133-139.

44. Hirota Y, Fujii T, Sano Y, Iyama S (1978) Nitrogen-fixation in rhizosphere of rice. Nature 276: 416-417.

45. Raad, II, Fang X, Keutgen XM, Jiang Y, Sherertz R, et al. (2008) The role of chelators in preventing biofilm formation and catheter-related bloodstream infections. Curr Opin Infect Dis 21: 385-392.

46. Thompson MG, Corey BW, Si Y, Craft DW, Zurawski DV (2012) Antibacterial activities of iron chelators against common nosocomial pathogens. Antimicrob Agents Chemother 56: 5419-5421.

47. van Asbeck BS, Marcelis JH, Marx JJ, Struyvenberg A, van Kats JH, et al. (1983) Inhibition of bacterial multiplication by the iron chelator deferoxamine: potentiating effect of ascorbic acid. European Journal of Clinical Microbiology & Infectious Diseases 2: 426-431.

48. Corbin BD, Seeley EH, Raab A, Feldmann J, Miller MR, et al. (2008) Metal chelation and inhibition of bacterial growth in tissue abscesses. Science 319: 962-965.

49. Paradkar PN, De Domenico I, Durchfort N, Zohn I, Kaplan J, et al. (2008) Iron depletion limits intracellular bacterial growth in macrophages. Blood 112: 866-874.

Biographical Sketch

Anthony Angotti was born on June 13, 1989 in Pittsburgh, Pennsylvania and attended Keystone Oaks High School. After graduating he went to Allegheny College where he double majored in Biology and Political Science and graduated in 2011. After receiving his M.S. degree he will pursue a career in laboratory equipment sales.